Chemical Physics Letters 462 (2008) 251–255

Contents lists available at ScienceDirect

Chemical Physics Letters

journal homepage: www.elsevier.com/locate/cplett

Potential energy surfaces for the lowest excited states of the nitrogen-vacancy point defects in diamonds: A quantum chemical study

A.S. Zyubin [a], A.M. Mebel [b,*], H.C. Chang [c], S.H. Lin [d]

[a] Institute of Problems of Chemical Physics, Russian Academy of Sciences, Chernogolovka, Moscow Region 142432, Russia
[b] Department of Chemistry and Biochemistry, Florida International University, 11200 SW 8th Street, Miami, FL 33199, USA
[c] Institute of Atomic and Molecular Sciences, Academia Sinica, P.O. Box 23-166, Taipei 106, Taiwan
[d] Institute of Molecular Sciences and Department of Applied Chemistry, National Chiao-Tung University, Hsin-chu, Taiwan

ARTICLE INFO

Article history:
Received 12 June 2008
In final form 18 July 2008
Available online 24 July 2008

ABSTRACT

Quantum chemical calculations of geometry relaxation in lowest excited states of neutral (NV^0) and negatively charged (NV^-) nitrogen-vacancy point defects in diamond have been performed employing the CASSCF method with a finite $NC_{19}H_{28}$ model cluster. Vibrations activated by the electronic transitions are determined by comparing calculated atomic displacements in the excited states with normal mode vectors, and the activated frequencies are evaluated as ~600 cm^{-1}. The barrier for N migration through the vacancy in NV^- is estimated at the TD-B3LYP level and no significant decrease of this barrier (~5 eV in the ground state) is found due to electronic excitations.

© 2008 Elsevier B.V. All rights reserved.

1. Introduction

Nitrogen-vacancy defects in diamonds, formed by aggregation of a vacancy and N impurity atoms (from one to three), are highly optically active. The remarkable properties of these diamond color centers, such as photo- and chemical stability, high quantum efficiency up to temperatures above 500 K, together with high thermal conductivity, outstanding hardness, and high damage threshold of the host crystal attracted substantial interest of researches [1,2]. The NV defect that is a combination of a single N atom and a vacancy exhibits a particularly strong electronic transition, allowing detection of individual centers optically [3]. These centers could be regarded as a good example of an individual quantum object with potential applications to the quantum information processing where a stable single-photon source with high quantum yield is required. Therefore, NV defects have been proposed as light sources for high-resolution scanning-probe microscopy and quantum cryptography [3–6]. Recently, nano-sized diamond powders containing NV-centers were also tested as cellular biomarkers [7].

According to the available experimental data [2,8], the neutral NV defect can capture an electron with formation of a negatively charged center. The ground electronic state of this NV^- center is $^3A_2$, and the first triplet excited state is ^3E. Maxima of the photo-adsorption (PA) and photo-luminescence (PL) bands have been observed near 2.15 and 1.75 eV with the zero phonon line (ZPL) at 1.945 eV [2,9]. The PL band appears to be well-structured, with a clear progression spaced by ~0.07 eV, but the PA band is less sharp and only the first phonon sideband at ~2.02 eV is clearly seen. Nevertheless, this spectral peak looks like a doublet split by ~0.01 eV. This peculiarity was explained based on the N tunneling model [9]. The key point in this approach is that the barrier for N migration through the vacancy in the excited electronic state is very low, of the same order of magnitude as the vibrational quantum for the observed progression. In the ground state of the NV^- center the N atom is connected with the neighboring atoms by means of three rather rigid N–C bonds, and switching the N and V positions should cause at least a large strain of these bonds up to their partial destruction. Hence, one can expect a high barrier for the N migration in the ground state of the NV^- center. The properties of potential energy surfaces (PES) can change significantly after electron excitations, however, it is difficult to judge a priory how drastically the first electronic transition will influence the barrier height for the nitrogen migration in the NV^- center.

Quantum chemical calculations of excited electronic states for this defect should be able to provide useful information in this case, but no data on excited state PES of NV^- are available so far in the literature. The existing publications devoted to theoretical studies of excited electronic states of this system considered only vertical excitations occurring at the ground state geometry. For instance, Goss et al. [10] used the cluster approach with a model system including about 70 atoms. The calculations were performed at the DFT level of theory within local spin density approximation (LSDA) and with a small Gaussian basis set. To evaluate the excitation energies, the authors used the Slater transition method. Luszczek et al. [11] employed self-consistent spin-polarized calculations within a generalized gradient approximation (GGA) using the full-potential linearized augmented plane wave (LAPW)

* Corresponding author. Fax: +1 305 348 3772.
E-mail address: mebela@fiu.edu (A.M. Mebel).

0009-2614/$ - see front matter © 2008 Elsevier B.V. All rights reserved.
doi:10.1016/j.cplett.2008.07.067

method with periodic boundary conditions, and the analysis of electronic states was carried out on the basis of Kohn–Sham eigenvalues. In our previous paper [12], we computed vertical transition energies to several excited states of NV^- and NV^0 at the CASSCF and CASPT2 levels in the frame of the cluster approach. The properties of PES for excited electronic states were not considered in these works. According to the available results, the lowest excited states for both defects involve non-bonding electrons from the vacancy-related C atoms and the N lone pair in the NV^0 system, whereas the electrons participating in the C–C and N–C bonds do not contribute into the transition. Therefore, one can hardly expect a substantial barrier decrease for the N–V transposition after excitation. Other features of the PES can change the mirror symmetry between the PL and PA bands and create additional peculiarities, such as change of the force constants, the Jahn–Teller effect, and non-linear coupling. [13]. Thus, in order to characterize the behavior of the system after excitation, one needs to unravel the properties of PES for excited electronic states, at least, the electronic and geometric structure of local minima on the surface and their rigidity. The aim of the present work is to investigate these properties for the lowest excited states of the NV^- and NV^0 centers employing high-level ab initio calculations.

2. Calculation details

Quantum chemical simulations of a diamond fragment containing NV-defects were carried out with the same three types of model clusters as in our previous work [12] with termination of broken boundary bonds by H atoms, $C_{19}NVH_{28}$, $C_{33}NVH_{36}$, and $C_{49}NVH_{52}$ (A1, A2, and A3, respectively, see Fig. 1). Geometric parameters for the ground states optimized at the B3LYP level [14] with the B1 basis set (the 6-31+G* basis set for atoms from the first shell around the vacancy, 6-31 G* for the atoms from the second shell, and 6-31G for others) were taken from our previous work [12]. Since the geometry optimization was performed keeping positions of boundary atoms taken from optimized defect-less clusters frozen, vibrational frequencies in the ground state minima were computed at the same theoretical level utilizing the Gaussian-03 program package. In the frequency calculations, the masses of boundary atoms were taken to be very high (∼10 000 amu), so that their displacements in the normal modes involving atoms from the inside cluster regions were insignificant.

Optimization of excited state geometries was carried out at the complete active space self-consistent-field (CASSCF) [15,16] level using the MOLPRO program package [16]. We used the B2 basis set for these calculations, which included the B1 basis set augmented by diffuse s-functions (with the same exponent as in 6-31+G) at the atoms from the second shell around the vacancy. Due to computer limitations only the $C_{19}NVH_{28}$ cluster was used for the calculations of excited states. The CASSCF calculations for the NV^- system were performed with two active spaces, (8,11) and (4,11), where eight or four electrons were distributed at 11 active molecular orbitals (MOs). These active spaces were found earlier to be the most suitable for describing the excited state under consideration [12]. The (8,11) active space covers orbitals with occupation numbers from 1.98 to 0.002; a shift of the active window down by several MOs results in non-equivalent contributions into the active space of the N–C and C–C bonds around the vacancy and hence does not provide better results. The (4,11) active space covers only those occupied MOs, which are constructed from broken bonds of the vacancy-related C atoms, as well as empty MOs with occupation numbers down to 0.0001. As was discussed in our previous work [12], the accuracy of the computed excitation energies is somewhat better with the (4,11) active space. Similar active spaces were also used for the ground state of the NV^0 defect, however, for the first excited state the active space choice is more complicated, as will be discussed in detail later.

3. Results and discussion

3.1. Geometry variations due to excitations and activated vibrations

As was discussed earlier [12], electronic transition from the ground state ($1^3A''$) to the 1^3E ($2^3A''$, $1^3A'$) and 5^3E ($6^3A''$, $5^3A'$) excited states was found to have the largest oscillator strengths for the NV^- defect. Therefore, for these states we optimized geometric parameters at the CASSCF level with the B2 basis set and two active spaces, (8,11) and (4,11). For comparison, the ground states geometries were also optimized. It appeared that the CASSCF results for the ground states are very close to the corresponding geometric parameters calculated at the B3LYP level [12] (see Tables 1 and 2). For the ground state of the NV^- defect the resulting geometry obtained at the CASSCF level is slightly distorted from C_{3v} symmetry, probably due to a limited active space (Table 2). This leads to slightly different distances of the C′ and C″ atoms from the vacancy center (Fig. 1). The difference is ∼0.006 Å with the

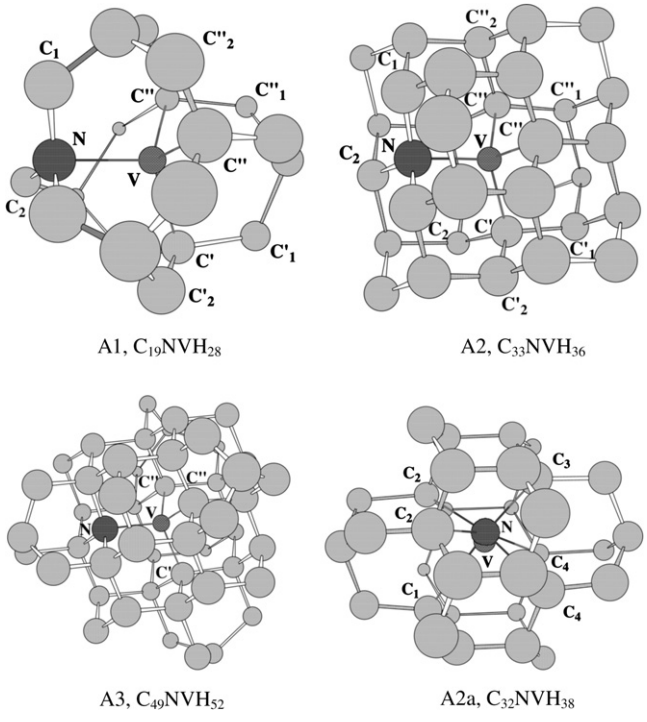

Fig. 1. Model clusters used for simulations of the nitrogen-vacancy (NV) defect in diamond (the boundary H atoms are not plotted).

Table 1
Interatomic distances R(AB), Å, in model clusters with NV defects in the ground electronic state calculated at the B3LYP level with the 6-31+G* basis set at central atoms 1–4, 6-31G* with diffuse s-function at atoms 5–16, and 6-31G at all other atoms

System[a]	R(VN)	R(VC)	R(NC′)	R(CC″)	R(VC′)	R(VC″)
A1, NV^-, t	1.88	1.79	1.47	1.50	2.54	2.54
A2, NV^-, t	1.69	1.66	1.48	1.49, 1.50	2.51	2.50, 2.51
A3, NV^-, t	1.67	1.63	1.49	1.51, 1.52	2.53	2.52, 2.54
A1, NV^0, d	1.82	1.79, 1.82	1.48	1.50–1.51	2.54	2.55
A2, NV^0, d	1.71	1.67	1.48	1.50, 1.51	2.51	2.51, 2.52
A3, NV^0, d	1.69	1.63, 1.66	1.51	1.51, 1.54	2.53	2.52, 2.54

[a] A1, A2, and A3 designate the $C_{19}NVH_{28}$, $C_{33}NVH_{36}$, and $C_{49}NVH_{52}$ model clusters, respectively, and t and d denote triplet and doublet electronic states.

Table 2
Interatomic distances R(AB), Å, in the NV^- and NV^0 defects in the ground and excited electronic states optimized at the CASSCF level using the $C_{19}NVH_{28}$ model cluster

State, active space, basis set[a]	VN	VC′	VC″	NC_1	NC_2	$C'C'_1$	$C'C'_2$	$C''C''_1$	$C''C''_2$
NV^-									
$1^3A''$, B3LYP	1.883	1.786	1.786	1.47	1.47	1.50	1.50	1.50	1.50
$1^3A''$, (8,11), B2	1.887	1.770	1.764	1.47	1.47	1.51	1.52	1.53	1.52
$1^3A'$, (8,11), B2	1.821	1.819	1.794	1.49	1.48	1.54	1.51	1.52	1.52
$2^3A''$, (8,11), B2	1.816	1.814	1.791	1.48	1.49	1.52	1.52	1.54	1.51
Averaged	1.818	1.816	1.792	1.48	1.48	1.52	1.52	1.53	1.52
$1^3A''$, (4,11), B2	1.886	1.765	1.769	1.47	1.47	1.51	1.52	1.51	1.52
$1^3A'$, (4,11), B2	1.823	1.820	1.790	1.49	1.48	1.52	1.52	1.53	1.52
$2^3A''$, (4,11), B2	1.817	1.801	1.812	1.48	1.49	1.52	1.52	1.52	1.52
Averaged	1.820	1.810	1.801	1.48	1.48	1.52	1.52	1.52	1.52
$5^3A'$, (4,11), B2	1.812	1.827	1.817	1.49	1.49	1.52	1.52	1.52	1.52
$6^3A''$, (4,11), B2	1.813	1.809	1.820	1.49	1.49	1.52	1.52	1.52	1.52
Averaged	1.812	1.818	1.818	1.49	1.49	1.52	1.52	1.52	1.52
NV^0									
$1^2A'$, (7,11), B2	1.844	1.825	1.781	1.48	1.48	1.52	1.52	1.53	1.52
$1^2A''$, (7,11), B2	1.843	1.774	1.806	1.48	1.48	1.52	1.53	1.52	1.52
Averaged	1.844	1.800	1.793	1.48	1.48	1.52	1.52	1.52	1.52
$1^2A'$, (3,11), B2	1.829	1.822	1.777	1.48	1.48	1.52	1.52	1.53	1.52
$1^2A''$, (3,11), B2	1.829	1.771	1.804	1.48	1.48	1.52	1.53	1.52	1.52
Averaged	1.829	1.796	1.790	1.48	1.48	1.52	1.52	1.52	1.52
$3^2A''$, (9,6), B1	1.885	1.832	1.733	1.51	1.52	1.52	1.51	1.53	1.51

[a] The B1 basis set includes 6-31+G* at N, C′, C″, 6-31G* at atoms 5–16, and 6-31G basis set at all other atoms. The B2 basis set is B1 + s(0.0438) at C atoms 5–16.

(8,11) active space and is slightly lower, ~0.004 Å, with (4,11) (Table 2). In general, the parameters optimized with the two active spaces are very close to each other, but the distortion from C_{3v} symmetry is smaller with (4,11).

Electronic excitations to the $2^3A''$ and $1^3A'$ states mainly lead to displacements of the vacancy-related N, C′, and C″ atoms. In particular, N is shifted towards the vacancy by ~0.07 Å, whereas C′ and C″ are shifted from the center by 0.03–0.05 Å (see Fig. 2 and Table 2). The coordinates of C atoms from the second shell around the vacancy (C_1, C_2, C_1', C_1'', C_2', and C_2'' in Fig. 1) are nearly unchanged. Deviations of the optimized structures from C_{3v} symmetry in these states are higher than for the ground state; the difference between V–C′ and V–C″ distances is ~0.02 Å with the (8,11) active space and 0.01–0.03 Å with (4,11). One can see that in this case the symmetry distortion is significant with both active spaces. Apparently, the 1^3E state, with components being $2^3A''$ and $1^3A'$, exhibits a weak Jahn–Teller distortion suppressed by rigidity of the neighborhood. Very similar results are obtained for the components of the second calculated PA band (the $5^3A'$ and $6^3A''$ states), but in this case the displacements of the nitrogen atom are somewhat smaller and those for C atoms are larger (Table 2, Fig. 2).

The atomic displacements following the $1^3A''$–1^3E and $1^3A''$–5^3E electronic transitions will activate atomic vibrations. We carried out vibrational frequency calculations for the ground state of the NV^- defect at the B3LYP level with the A2 and A3 model clusters to determine what kind of vibration will be triggered by these transitions. In both model systems, we found one particular vibrational mode with atomic displacements (Fig. 3) rather similar to the changes of atomic coordinates after the considered electronic transitions. The calculated frequency of this a′ normal mode is about 600 cm^{-1} or 0.074 eV (Fig. 3). This value is in good agreement with the observed spacing in the PL and PA bands corresponding to the NV^- defect in diamond [9]. In the smallest A1 cluster the corresponding normal mode with similar displacements has a lower frequency of ~430 cm^{-1}, because the force constants for displacements of vacancy-related atoms in radial directions are approximately twice lower for A1 as compared to the corresponding values for the A2 and A3 clusters (Table 3). The most probable reason of this difference is that in the A1 cluster such displacements lead mainly to deformations of C–C–H bond angles, whereas in the larger clusters more rigid C–C–C angles are deformed.

As frequency calculations for excited electronic states were not feasible, we estimated the rigidity of PES with respect to

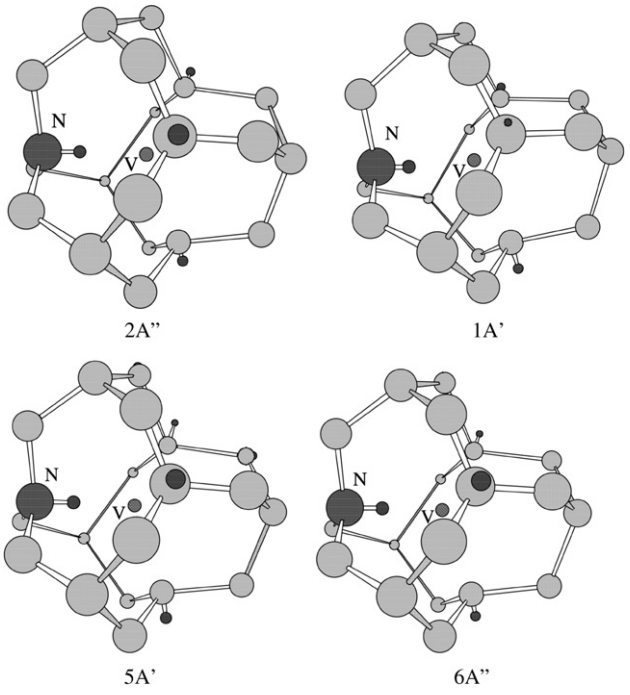

Fig. 2. Atomic displacements following electronic excitation in the NV^- defect. Small black circles show new atomic positions. The displacement vectors are 10-fold enlarged.

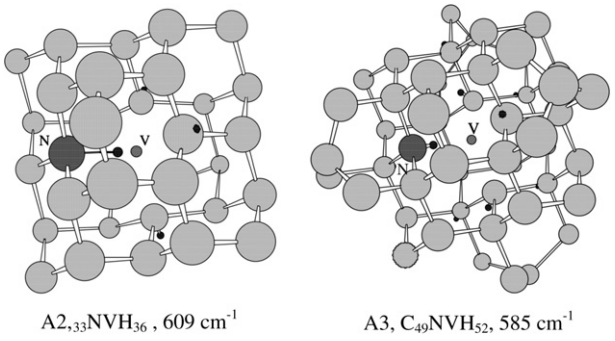

Fig. 3. Atomic displacements corresponding to the vibrational normal mode in the NV^- defect activated by the electronic transition. Small black circles show new atomic positions. The displacement vectors are twofold reduced.

Table 3
Evaluated force constants (eV/Å^2) for displacements of vacancy-related N and C atoms in radial directions in the NV^- defect in the ground and excited electronic states[a]

	$1^3A''$-TD[b], A1	$1^3A''$-TD[b], A2	$1^3A''$-TD[b], A3	$1^3A''$-CAS[c], A1	$1^3A'$-CAS[c], A1	$2^3A''$-CAS[c], A1
k(N)	11.4	23.2	27.7	11.4	11.9	12.4
k(C)	15.4	28.9	26.4	14.2	13.9	15.3

[a] A1, A2, and A3 denote the $C_{19}NVH_{28}$, $C_{33}NVH_{36}$, and $C_{49}NVH_{52}$ model clusters, respectively.
[b] From TD-B3LYP calculations.
[c] From CASSCF calculations.

displacements of the vacancy-related atoms in radial directions using finite-differences force constant calculations (see Table 3). The calculated force constants appeared to be similar for the ground and excited states ($1^3A''$, $1^3A'$, $2^3A''$) and therefore the vibrational frequencies activated by the electronic transition should be alike in the PL and PA bands. The same conclusion can be made from calculations of energy differences between the geometric structures optimized for the ground and excited states. For instance, the energy of the ground electronic state increases, as compared to its local minimum, by 0.067 and 0.080 eV at the geometries optimized for the excites $1^3A'$ and $2^3A''$, respectively (CASSCF(4,11) results in Table 4). And vice versa, the energies of the $1^3A'$ and $2^3A''$ excited states increase by 0.077 and 0.084 eV, respectively, at the geometry optimized for the ground state. Thus, similar geometric changes in the ground and excited states result in similar energetic variations, indicating that the PESs have similar curvature. Interestingly, the calculated energy changes are too low, in the same order of magnitude as one vibrational level, whereas the observed PL and PA bands are peaked at the third vibrational level above ZPL. Apparently, the CASSCF calculations somewhat underestimate the atomic displacements in the excited states, which may be caused by substantial undervaluation of excitation energies by this method for the clusters simulating the NV^- defect [12].

For the neutral doublet NV^0 defect in the ground state, the geometric distortion from C_{3v} symmetry is more significant than for NV^- due to the Jahn–Teller effect, so as this state originates from doubly degenerate ^2E. The deviations concern mainly distances between the vacancy center and the vacancy-related C atoms, with differences of 0.02–0.04 Å. Depending on the state being optimized, $1^2A'$ or $1^2A''$, the deviations have opposite signs and almost equal values, so that the averaged geometry is very close to a C_{3v}-symmetric structure (Table 2). Because the two components should roughly be equally populated, the mean geometry of NV^0 in the 1^2E state will probably exhibit C_{3v} symmetry.

As was discussed earlier [12], the account of dynamic electronic correlation in the NV systems results in a substantial decrease of relative energy for the $1A_2$ state. For the neutral defect, this causes a change in the relative order of electronic states as calculated by the CASSCF and CASPT2 methods. To correctly reproduce the excitation energy and wave function of the second excited state for NV^0 (the first state above the two $1^2A'$ and $1^2A''$ components of 1^2E and hence from thereon we will refer to this state as the first excited state), one has to select from the initial CASSCF calculation the state involving electron transfer from the two highest doubly occupied molecular orbitals HOMO-1 and HOMO to the singly-occupied SOMO orbital [12]. Unfortunately, at the CASSCF level the required state is higher in energy than numerous states involving transitions to diffuse orbitals and therefore one needs to exclude or limit participation of these states in the CASSCF calculation to ensure that the state corresponding to the HOMO-1/HOMO→SOMO transition is available. This can be achieved by using a basis set with a moderate amount of diffuse functions (6-31+G* at the vacancy-related atoms only) and with a limited (9,6) active space [12].

Table 4
Relative energies (eV) of geometric structures optimized for the ground and excited electronic states with respect to local minima in the corresponding states for the NV^- point defect, calculated at the CASSCF level with the $C_{19}NVH_{28}$ model cluster and B2 basis set

Active space	$1^3A''$ at $1^3A'$ [a]	$1^3A''$ at $2^3A''$ [a]	$1^3A'$ at $1^3A''$ [a]	$2^3A''$ at $1^3A''$ [a]
(4,11)	0.067	0.080	0.077	0.084
(8,11)	0.074	0.088	0.079	0.095

[a] The first term designates the electronic state for which the energy was calculated and the second term shows the electronic state for which the geometry was optimized.

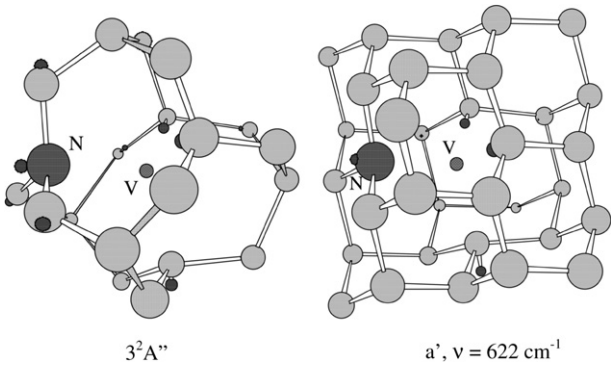

Fig. 4. Atomic displacements following electron excitation and the corresponding vibrational normal mode in the NV^0 defect. Small black circles show new atomic positions. The displacement vectors corresponding to geometry relaxation after electronic excitation are 10-fold enlarged.

The resulting CASPT2 wave function for the first excited 1^2A_2 state is multi-reference, with the maximal coefficient (~0.7) corresponding to the $3^2A''$ state from the CASSCF wave function. Therefore, to evaluate the geometry relaxation in the first excited state of the NV^0 defect, we optimized geometry of the $3^2A''$ state at the CASSCF(9,6) level with the B1 basis set (Table 2). One can see that atomic displacements in this state distort C_{3v} symmetry, as one of the vacancy-related C atoms is shifted away from the vacancy, but the other two move toward the vacancy (Fig. 4). Additionally, the N atom moves away from the vacancy and some of the C atoms from the second shell also exhibit noticeable displacements. The normal mode in the ground electronic state, which most closely reproduces the atomic displacements described above, has vibrational frequency of ~622 cm^{-1} and a' symmetry (Fig. 4). Therefore, one can expect similar vibrational spacing of about 600 cm^{-1} in the bands corresponding to the NV^- and NV^0 defects. However, for NV^0 the vibronic band can be expected to be more diffuse (less structured) due to the mixing of states in the resulting 1^2A_2 wave function and also to a not very perfect match between the atomic displacements resulting from the electronic excitation and those in the activated a' vibrational mode, meaning that other normal modes may also be turned on by the excitation.

3.2. Barrier for N migration

The transition state structure for the N atom migration through the vacancy in the NV^- defect was optimized using the $C_{32}NVH_{38}$ model cluster (Fig. 1). Boundary atoms were kept frozen as in a defect-less system and coordinates of the vacancy-related N and C_1–C_4 atoms were varied. In the transition state, the N atom is found to be located near the cavity center, but it is slightly shifted (by ~0.2 Å) from the C_{3v} axis. As a result, the N–C distances are non-equivalent and vary from 1.76 and 1.94 Å for N–C_3 and N–C_2 to 2.16 and 2.31 Å for N–C_4 and N–C_1, respectively. Thus, at the barrier position the C–N bonds are significantly stretched, by up to 0.3–0.4 Å. Because these bonds are rather rigid, their stretching leads to the energy increase of 4.94 eV relative to the equilibrium structure. It is worth noting that the S^2 value in the transition state region remains close to 2.0, as in the ground state minimum, and there is no complete bond destruction near the barrier; some new N–C are being formed while the old bonds are being cleaved.

In the lowest excited states of the NV^- defect broken bonds from the vacancy-related C atoms are involved in the electron density redistribution, whereas the electron density from the N–C and C–C bonds does not contribute to these electronic transitions. Therefore, the barrier position in the lowest excited state should not change significantly as compared to that in the ground state

and one can use the ground state TS geometry to estimate the barrier on the excited state PES. Within this approximation we computed the barrier heights for the two lowest excited states of the NV^- defect. Calculations at the TD-B3LYP level with the basis set including 6-31+G* at five inner atoms (N and C_1–C_4) and 6-31G at all other atoms show that the excitations result in a rather moderate barrier decrease and the barriers remain high, of 4.29 and 4.43 eV in the $1^3A'$ and $2^3A''$ excited states, respectively. Despite the approximate character of these estimations, it is clear that the barrier for the migration of the N atom through vacancy in the lowest excited state is much higher than the vibrational energy of the normal mode activated by this transition. Therefore, the ascription of the vibrational level splitting to tunneling of the N atom [9] is not confirmed by these calculations. Also, it is worth noting that if the N tunneling motion does occur, it would result in a significant decrease of the vibrational spacing in the PA band (by a factor of ~1.5) [9], however there is no evidence for such effect in the experimental spectra. Obviously, another reason for the splitting of the vibrational levels in the PA band needs to be searched for. A possible mechanism might be indirect activation of low-frequency vibrations of e-type causing weak Jahn–Teller splitting of the degenerate excited state.

3.3. Concluding remarks

Quantum chemical calculations of geometry relaxation in the lowest excited states of the neutral and anionic nitrogen-vacancy point defects in diamonds demonstrate moderate displacements of the atoms surrounding the vacancy, including nitrogen and three tri-coordinated carbons. Atomic shifts in the next coordination layer appear to be much smaller. In the negatively charged NV^- defect the N atom is shifted toward the vacancy center after electronic excitation and the C atoms exhibit opposite displacements away from the vacancy, so that symmetry of the system remains unchanged. Alternatively, the first electronic excitation in NV^0 leads to non-equivalent displacements of the vacancy-related C atoms, which break the cluster symmetry. Vibrational frequency and normal mode vector calculations for both model systems demonstrate, in comparison with the atomic displacements following electronic excitations, that the lowest transitions should activate normal modes with a frequency of about 600 cm^{-1}, in reasonable agreement with the vibrational spacing observed in the experimental PA and PL bands due to the NV defect. Estimated curvatures of the potential energy surfaces along the activated vibrational mode for the ground and excited states are similar and, as a result, the vibrational spacing in the PA and PL bands should be close. It is also found that the lowest excitations do not cause substantial decrease of a high barrier for the N migration through the vacancy in the NV^- system (about 5 eV in the ground state), and therefore the attribution to splitting of the vibration level in the PA band for this system by tunneling of the N atom is not confirmed by the present calculations.

Acknowledgments

The authors acknowledge Academia Sinica and National Science Council of Taiwan, ROC for financial support. A partial support from Florida International University is also appreciated.

References

[1] S.C. Rand, L.G. DeShazer, Opt. Lett. 10 (1985) 481.
[2] F. Jelezko, C. Tietz, A. Gruber, I. Popa, A. Nizovtsev, S. Kilin, J. Wrachtrup, Single Mol. 2 (2001) 255.
[3] C. Kurtsiefer, S. Mayer, P. Zarda, P. Weinfurter, Phys. Rev. Lett. 85 (2000) 290.
[4] J. Martin, R. Wannemacher, J. Teichert, L. Bischoff, B. Kohler, Appl. Phys. Lett. 75 (1999) 3096.
[5] R. Brouri, A. Beveratos, J.-P. Poizat, P. Grangier, Phys. Rev. A 62 (2000) 0683171.
[6] N. Gisin, G. Ribordy, W. Tittel, H. Zbinden, Rev. Mod. Phys. 74 (2002) 145.
[7] S.J. Yu, M.W. Kang, H.C. Chang, K.M. Chen, Y.C. Yu, J. Am. Chem. Soc. 127 (2005) 17604.
[8] Y. Mita, Phys. Rev. B 53 (1996) 11360.
[9] G. Davies, M.F. Hamer, Proc. Roy. Soc. London A 348 (1976) 285.
[10] J.P. Goss, R. Jones, S.J. Breuer, P.R. Briddon, S. Öberg, Phys. Rev. Lett. 77 (1996) 3041.
[11] M. Luszczek, R. Laskowski, P. Horodecki, Physica B 348 (2004) 292.
[12] A.S. Zyubin, A.M. Mebel, M. Hayashi, H.C. Chang, S.H. Lin, Quantum chemical modeling of photo-adsorption properties of the nitrogen-vacancy point defect in diamond, J. Comput. Chem., in press. <http://www3.interscience.wiley.com/cgi-bin/fulltext/119818666/PDFSTART>.
[13] J. Walker, Rep. Prog. Phys. 42 (1979) 1605.
[14] M. J. Frisch et al., Gaussian 03, Revision B.03, Gaussian, Inc., Pittsburgh, PA, 2003.
[15] H.-J. Werner, P.J. Knowles, J. Chem. Phys. 82 (1985) 5053.
[16] Molpro is a package of ab initio programs written by H.-J. Werner and P. J. Knowles with contributions from R. D. Amos et al., Molpro version 2002.6, University of Birmingham, Birmingham, UK, 2003.